ELSEVIER

Journal of Molecular Catalysis A: Chemical 117 (1997) 57–70

JOURNAL OF MOLECULAR CATALYSIS A: CHEMICAL

Oxidation catalysis with semi-inorganic zeolite-based Mn catalysts

Peter-Paul Knops-Gerrits, Dirk E. De Vos, Peter A. Jacobs *

Center for Surface Chemistry and Catalysis, Katholieke Universiteit Leuven, Kardinaal Mercierlaan 92, B-3001 Heverlee, Belgium

Received 4 July 1996; accepted 13 August 1996

Abstract

The chelation of zeolite-exchanged Mn^{2+} by N-containing ligands gives rise to a whole class of heterogeneous liquid phase oxidation catalysts. Bi-, tri- or tetradentate ligands can be used. A high degree of metal complexation is required to avoid side reactions due to the presence of zeolite-coordinated manganous ions. Applied physico-chemical techniques include IR, ESR and electronic spectroscopy. Oxidation-resistant chelands, e.g. with aromatic pyridine groups, are employed to ensure long-term catalyst stability. Use of hydrogen peroxide is most successful in combination with 2,2′-bipyridine (bpy) or 1,4,7-trimethyl-1,4,7-triazacyclononane (tmtacn); with both systems double bond oxidation proceeds with high selectivity. Olefin oxidations with other oxidants, e.g. *tert*-butylhydroperoxide (*t*BuOOH) or iodosylbenzene, are less selective or slower. Alkane oxidation with *t*BuOOH is possible with various tetradentate diimine ligands. A principal effect of the zeolite matrix is that formation of Mn clusters is impeded in comparison with solution chemistry. Other effects of the zeolite matrix include modulation of the acid strength and suppression of side reactions, such as allylic oxidation of olefins or formation of isomerized epoxides.

1. Introduction

The intense present interest in the redox chemistry of Mn relies on the role of Mn in numerous metallo-enzymes. In biological systems, Mn may be present as a mononuclear complex, as a dimer or as a cluster of higher nuclearity (e.g. in Photosystem II) [1]. The mimicking of these enzymes has grown into an inorganic synthetic challenge on itself, with spin-offs e.g. in the development of very high spin transition metal aggregates [2]. In these clustering reactions, anion and solvent play a crucial role [3]. For instance, acetate is well-known to promote bridging between Mn atoms, as in manganic acetate; working with permanganate in ethanol instead of in water prevents formation of MnO_2 precipitates.

Zeolite lattices with their net negative charge can serve both as a solvent and as a counter-anion to complexes of metal cations. Consequently profound effects of the zeolite lattice on the oxidative chemistry of entrapped Mn complexes may be expected. Not only the nuclearity of the formed complexes can be different; the changes may also be expressed in the redox and catalytic properties of the encapsulated Mn complexes.

* Corresponding author.

PII S1381-1169(96)00358-5

This basic idea formed the incentive to study the properties of Mn zeolites, with ligands adsorbed in the micropores of the framework. Used ligands are compiled in Fig. 1. The synthetic flexibility in the design of polypyridines, polyamines, polyamides and Schiff bases was fully exploited. In this paper, an overview is given of the physico-chemical understanding of these systems, followed by a detailed discussion of the catalytic behavior in selective oxidations. Both literature data and new data from our laboratory are discussed.

2. Catalyst preparation and apparatus

2.1. General procedure

Catalysts are prepared by adsorption of a N-containing ligand on a Mn zeolite. The exchange of e.g. NaY with Mn^{2+} is performed in 2 mM solutions of Mn^{2+} at a pH between 5 and 6. At this pH, oxidation of Mn^{2+} to Mn^{3+} and hydrolysis of Mn^{2+} are negligible. However, proton exchange cannot be excluded, and effects of acidity can be expected. After air dry-

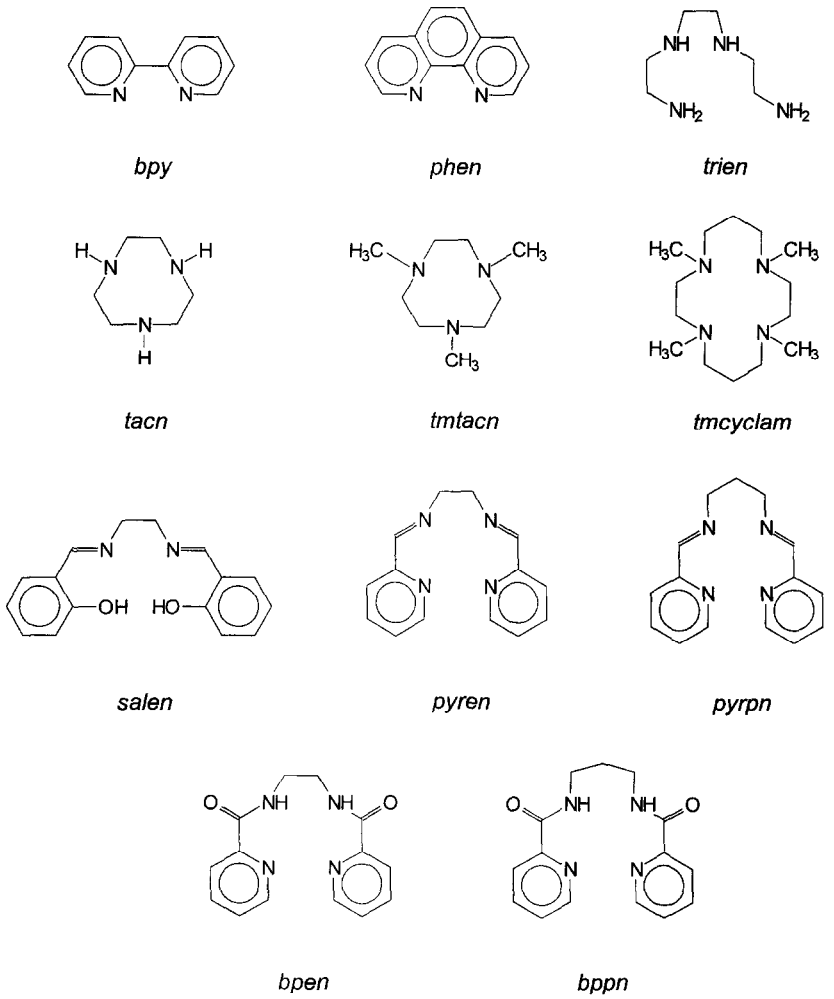

Fig. 1. Chemical formulae of the ligands in the zeolite-based Mn redox catalysts.

ing, the zeolites are dehydrated in a flow of N_2 under slow heating till a final temperature of 423–673 K. Water-sensitive ligands, such as Schiff bases, require in general a deeper dehydration of the zeolite than e.g. polypyridines. Finally, the dried zeolite is mixed with the water-free ligand and heated to stimulate adsorption of the ligand into the micropores. This heating is performed under vacuum or inert atmosphere in a *closed* glass vessel, which impedes loss of ligand by evaporation or sublimation. The heating duration and temperature depend on the thermal stability of the ligand. While e.g. bipyridine is highly stable, heating of cyclic triamines is limited to 10 h in order to avoid cycle degradation by elimination reactions. Organic ligands were purchased commercially or were synthesized. Their identity and purity were controlled by ^1H NMR spectroscopy. Examples of not previously described syntheses are given below.

2.2. Synthesis of N,N'-bis(2-pyridinecarboxamide)-1,2-ethane (bpen) [4]

To a solution of 2-pyridinecarboxylic acid (12.3 g, 0.1 mol) in 40 ml pyridine, 3.0 g 1,2-diaminoethane (0.05 mol) in 10 ml pyridine is added. After 10 min stirring, a white precipitate forms and the suspension is heated on an oil bath. 26.2 ml of triphenylphosphite (0.1 mol) is slowly added and the solution is refluxed for 4 h. Cooling yields a yellow precipitate. After recrystallisation from ethanol, white–yellow needles are obtained (m.p. 190°C).

2.3. Synthesis of N,N'-bis(2-pyridinecarboxamide)-1,3-propane (bppn)

The procedure is analogous to that for bpen, but instead of ethylenediamine, 3.7 g of 1,3-diaminopropane is added. Overnight crystallisation and recrystallisation from ethanol gives white crystals (m.p. 91°C).

2.4. Synthesis of $[Mn(phen)_2]^{2+}$–NaY

The method is analogous to that reported for *cis*-$[Mn(bpy)_2]^{2+}$–NaY [5]. Following stoichiometry results in a zeolite with 1.7 wt% of Mn, or 1 Mn per 2 supercages. 1.3 g of NaY zeolite (on dry weight basis) is stirred in 200 ml of a 2 mM aqueous $Mn(CH_3COO)_2$ solution. After repeated washing, the zeolite is dried for 15 h at 423 K in a N_2 flow of 100 ml per minute. In a N_2 glovebox, 1 g of the dehydrated MnNaY is intimately mixed with 0.14 g 1,10-phenantroline (phen) ligand, which corresponds to a phen:Mn ratio of 2.5:1. This mixture is kept at 363 K for 24 h and Soxhlet-extracted for 24 h with CH_2Cl_2 to remove unreacted ligand.

2.5. Synthesis of [Mn(bpen)]–NaY and [Mn(bppn)]–NaY

An analogous procedure is followed but the zeolite is dehydrated at 473 K before ligand addition. To 1 g of dry zeolite, 0.091 g of bpen or 0.096 g of bppn is added, corresponding to a 10% ligand excess with respect to Mn. After a 96 h adsorption at 393 K and Soxhlet extraction, grey (bpen) or yellow–brown (bppn) samples are obtained.

2.6. Apparatus

ESR spectra were recorded at X-band with a Bruker ESP-300 with a TE_{104} cavity. ESCA measurements were performed with a Perkin-Elmer PHI 5500-5600 instrument with monochromatic AlKα X-radiation (1486.6 eV). Calibration values are: $Mn(2p_{3/2})$: 639.6 eV (sensitivity factor 150.146); Al(2p): 71.2 eV (SF 19.719); Si(2p): 99.7 eV (SF 28.827). FT-IR spectroscopy was performed on a Nicolet FT-IR 730, averaging 400 scans per sample. Diffuse reflectance UV–VIS–NIR spectra were recorded on a Cary-5 with a $BaSO_4$ coated integration sphere. Catalytic reactions were performed in stirred glass vessels, equipped to operate under cooling or gradual reactant addition.

3. Physico-chemical characterization of ligand-containing Mn zeolites

3.1. Electron spin resonance spectroscopy

ESR can probe the nuclearity, the valency and especially for divalent Mn, the local symmetry. The latter information can be derived from the values of the parameters D and E, which describe the splittings between the 6 energy levels for an $S = 5/2$ cation in zero magnetic field [6]. For unchelated Mn^{2+} in faujasite type zeolites, D and E are quite small, so that only the $\Delta M_S = +1/2 \leftrightarrow -1/2$ transition is observed, with the other four non-Kramers transitions broadened and hidden under this central band [7]. A distortion of the symmetry from this originally close-to-octahedral state gives rise to supplementary lines, both upfield and downfield from the central transition, due to the transitions involving the $M_S = +5/2$, $+3/2$, $-3/2$ and $-5/2$ states. Moreover, the intensity of the half-field transitions ($\Delta M_S = \pm 2$) increases exponentially with the magnitude of the zero-field splitting; this yields a new feature centered around $g = 4.3$ [8]. In the case of axial symmetry, $D \neq 0$ and $E = 0$, and the value of D may be derived directly from the spacing between the 5 fine lines [6]. For instance, ligands of the triazacyclononane type (tacn and tmtacn), adsorbed on MnNaY, produce such spectra [9]. For lower symmetry, e.g. with *cis*-[Mn(bipyridine)$_2$]$^{2+}$, the non-zero value of E causes an additional splitting.

These trends are illustrated in Fig. 2a and b for a MnNaY zeolite containing bipyridine (bpy) or tetramethylcyclam (tmcyclam, 1,4,8,11-tetramethyl-1,4,8,11-tetraazacyclotetradecane). For relatively small values of D and E, most of the spectral intensity in X-band remains accumulated close to the $g_{eff} = 2$ value, as observed for the bpy containing sample [10]. The spectral features outside this central domain get much more important with tmcyclam. The half-field transition is prominent, and non-Kramers transitions are well-recognizable, e.g. at 2600, 3800 and 4700 G. If there is a distribution of D values, or if D and E get large, less resolved spectra may be obtained and a complex, often broad spectrum is obtained. Thus, even if it is not always possible to assign unambiguously the symmetry of the formed Mn complexes based on the ESR spectrum, the observation of lines outside the central sextet gives at least a semi-quantitative idea on the distortions caused in the Mn coordination sphere by the adsorbed ligand.

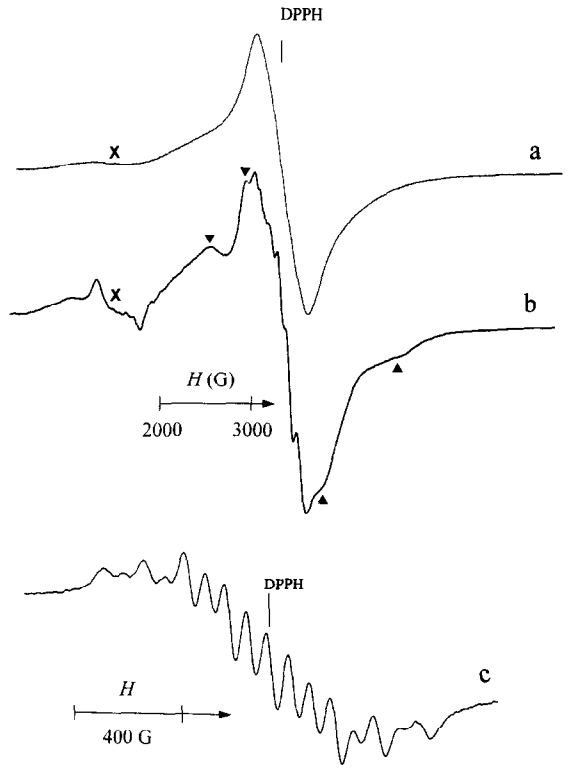

Fig. 2. X-band ESR spectra (120 K) of (a) [Mn(bpy)$_2$]$^{2+}$–NaY, (b) [Mn(tmcyclam)]$^{2+}$–NaY. For (a), the spectrum remained the same after long exposure to ambient air. (×) indicates the half-field transition (at $g_{eff} = 4.3$). In (b), (▲) indicate the non-Kramers transitions, involving $S = 5/2$, $3/2$, $-3/2$ or $-5/2$ states. (c) Spectrum of air-exposed [Mn(trien)]$^{2+}$–NaY, with the 16-line signal of a Mn^{III}–Mn^{IV} dimer.

The zeolite encapsulation has also an impact on the nuclearity and valency. To evaluate the amount of Mn^{II} in a sample, the room temperature ESR spectrum of a known amount of Mn zeolite is integrated twice. This prevents interference by other, high valent species, which

only become visible at low temperature. For a $[Mn(bpy)_2]^{2+}$–NaY zeolite, the intensity of the Mn^{II} signal is not affected by exposure to air. This sharply contrasts with the behaviour of $[Mn(bpy)_2]^{2+}$ complexes in aerated solution, where oxidation and dimerization take place. The latter phenomena are characterized by the observation at $T < 150$ K of a 16-line signal of a Mn^{III}–Mn^{IV} dimer [11], though other redox and aggregation states may also occur. A similar 16-line signal is observed upon exposure of a $[Mn(trien)]^{2+}$–NaY zeolite to air (see Fig. 2c; trien = triethylenetetramine). The observation of the latter dimer implies that the $[Mn(trien)]^{2+}$ complexes are sufficiently small or flexible to migrate through the 12-MR windows of the zeolite and form dimers. In contrast, the $[Mn(bpy)_2]^{2+}$ chelates are too large to allow complex diffusion through the pore system, and this secures the mononuclear character of the complex.

3.2. *Diffuse reflectance spectroscopy*

In the spectra of ligand containing Mn zeolites, one would expect the d–d transitions from the $^6A_1$ ground state of high spin Mn^{II} to higher lying states [12]. However these are mostly masked by more intense transitions. For bpy and phen containing zeolites, charge transfer

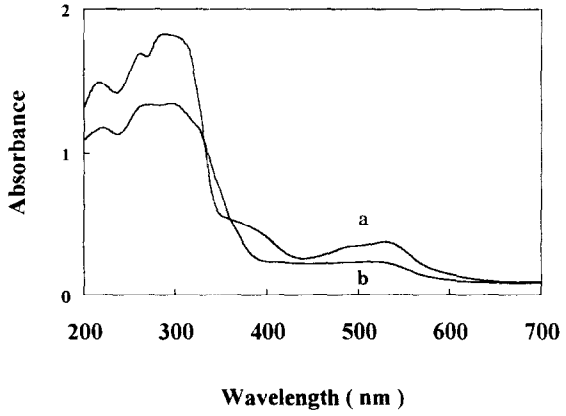

Fig. 3. Diffuse reflectance spectra of (a) $[Mn(bpy)_2]^{2+}$–NaY, and (b) $[Mn(phen)_2]^{2+}$–NaY.

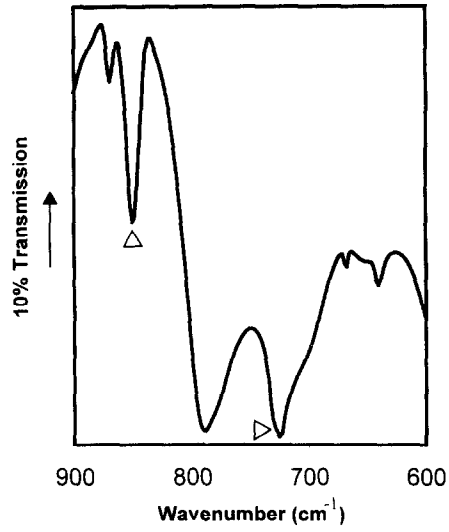

Fig. 4. FT-IR spectrum of $[Mn(phen)_2]^{2+}$–NaY in the 600–900 cm^{-1} region. (△) indicate the C–H out-of-plane deformation vibrations of the phen ligand.

bands are observed, which originate in the MLCT case from the promotion of an electron from the metal to the ligand, resulting in a ^5D Mn^{III} state [13]. Significant differences are observed between the charge transfer bands of nay entrapped $[Mn(phen)_2]^{2+}$ and $[Mn(bpy)_2]^{2+}$ (Fig. 3). With the phen ligand, the MLCT bands (at 524 and 480 nm) are significantly broader than with bpy (530 and 486 nm). This difference follows from the different degree of distortion of the coordination sphere for both compounds. With the flexible bpy ligand, rotation along the C_2–C'_2 axis is allowed, but with the rigid phen molecule, no deviation from the planar ligand structure is possible. As a result, the phen ligand is less capable of adapting to different coordination requirements, and distortions of the coordination sphere are more pronounced with phen than with bpy. Strong charge transfer bands are also observed for other Mn zeolites containing α-diimine ligands, such as the Schiff bases pyren and pyrpn (pyren = bis(2-pyridinecarboxaldehyde)-1,2-ethylenediimine; pyrpn = bis(2-pyridinecarboxaldehyde)-1,3-propylenediimine) [14]. The latter materials display a purple color, and absorb strongly around 600 nm.

In the UV domain, the $\pi-\pi^*$ transitions of aromatic ligands are dominant. For instance for $[Mn(phen)_2]^{2+}$–NaY, the 226, 265 and 290 nm absorptions are characteristic for the metal-coordinated ligand. However, it cannot be excluded that part of the phen ligand, with $pK_1 = 4.98$, is present in its protonated form, which is expected to absorb at 222 and 276 nm [13].

3.3. Fourier transform infrared (FT-IR) spectroscopy

In the case of the polypyridine ligands, IR can be used to probe the stereochemistry of the intrazeolite complexes. To discriminate between *cis* and *trans bis* complexes, the C–H out-of-plane (oop) deformation vibrations are employed [15]. For $[Mn(bpy)_2]^{2+}$–NaY, a splitted band is observed around 765 cm^{-1}. Such a splitting is also observed for crystalline $[Mn(bpy)_2(NO_3)_2]$ with *cis* conformation, but not for the analogous, more symmetrical *trans* complex. Hence the intrazeolite complex has the *cis* conformation [5]. A similar argument applies to the phen system. In the relevant domain, two discrete absorptions are observed, around 725 and 848 cm^{-1}, which can both be assigned to ring H atoms moving in phase out of the plane of the aromatic ring. As the frequency of such vibrations increases with a decreasing number of adjacent H atoms on the ring, the 848 cm^{-1} band is assigned to the oop

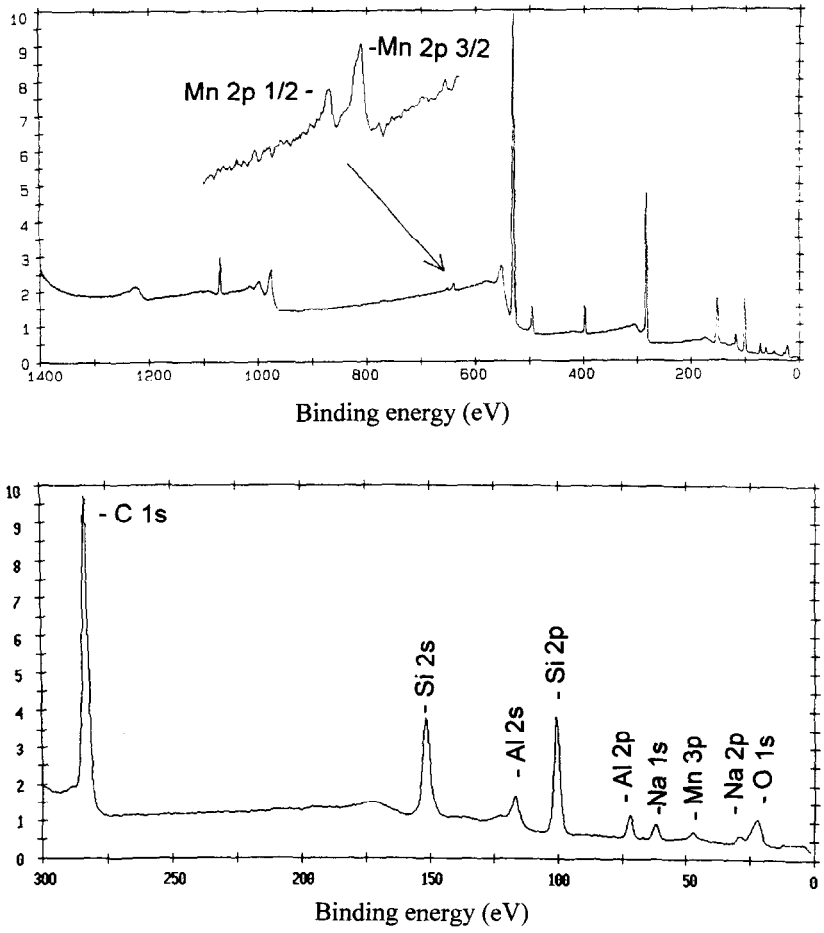

Fig. 5. ESCA data for $[Mn(phen)_2]^{2+}$–NaY: (upper spectrum) survey scan of the 0–1400 eV region with magnified insert of the 600–700 eV region and (bottom spectrum) the 0–300 eV region.

motion of H on the central ring (with two neighboring H atoms) and the 725 cm^{-1} band to that of the pyridyl rings, where there are three adjacent H atoms (Fig. 4). Again these bands are degenerate for the highly symmetrical crystalline *trans* compound (D_{2h}), but for the crystalline *cis* complex (C_2) and for the zeolite-entrapped compound, especially the low-frequency oop vibration displays a discernable splitting. This allows to assign a *cis* conformation to the zeolite-occluded complex.

3.4. Surface analysis

The Mn distribution in the zeolite crystal can be assessed via a combination of ESCA, elemental analysis, thermogravimetry and electron microscopy. This is illustrated by the data for a $[Mn(phen)_2]^{2+}$–NaY sample, prepared with a loading of 1 Mn ion per supercage. Already the SEM pictures do not allow to detect any other material than crystalline faujasite. With ESCA (Fig. 5) and elemental chemical analysis (CA), following elemental ratios are found: Mn:Si = 0.044 (ESCA) and 0.06 (CA); Mn:Al = 0.18 (ESCA) and 0.14 (CA). From these numbers a surface enrichment of Si with respect to Al can be deduced, which is in agreement with earlier ESCA work on zeolites [16]. However, if all tetrahedral lattice atoms (T) are considered together, the Mn:T ratio at the surface closely matches that in the crystal bulk, proving that complexation is mainly an inner pore process. With thermogravimetric analysis, a phen:Mn ratio of 2.14:1 is obtained. The corresponding N:Mn ratio is only slightly lower than that obtained by ESCA (N:Mn = 5.12). Thus ligand accumulation in the outer rim of the crystals seems insignificant.

4. Selective catalytic oxidation

4.1. Bidentate ligands

The occlusion of $[Mn(bpy)_2]^{2+}$ and related complexes in faujasites is a revealing example of the potential beneficial effects of zeolite entrapment on the catalytic properties of a metal compound [5,17]. As demonstrated via ESR, the occlusion of $[Mn(bpy)_2]^{2+}$ in the supercages renders the complex resistant against oxidative processes such as the formation of μ-oxo di- or trimers. While these clusters are inactive in catalytic oxygenation, the monomeric, zeolite-occluded species permits selective alkene oxygenation with H_2O_2. In the zeolite, $[Mn(bpy)_2]^{2+}$ and Brønsted acid sites can be intimately mixed. This bifunctionality allows to open the epoxides formed on the Mn sites. Starting from cyclic alkenes, either epoxides or further oxidation products, such as α,ω-alkanedicarboxylic acids, can be obtained in one step (Table 1) [18].

One would expect the hydrophilic nature of the host material to prevent diffusion of the olefin substrate towards the active Mn sites. This would be the case if one would be dealing with a simple NaX or NaY zeolite. In ligand

Table 1
Substrate conversions (X, %) and product selectivities (S, %) in the oxidation of alkenes and styrenes with $[Mn(bpy)_2]^{2+}$, encapsulated in faujasites [a]

Substrate	Host	X (%)	S (%)		
			epoxide	diol	diacid
1-hexene	NaY	20	50	40	—
Cyclohexene	NaY	62	6	79	—
Cyclohexene [b]	NaY	100	—	—	80
1-hexene [c]	NaX	22	81	14	—
Cyclohexene [c]	NaX	41	62	32	—

Substrate	Host	X (%)	S (%)		
			epoxide	diol	PhCXO
Styrene	NaY	21	81	1	11 [d]
E-β-CH_3-styrene	NaY	31	39 [e]	1	39 [d]
α-CH_3-styrene	NaY	43	23	2	73 [f]

[a] Reaction conditions: 60 mmol of 1-hexene or cyclohexene, 120 mmol H_2O_2, 0.2 mmol Mn in 0.3 g catalyst, 50 ml acetone, 18 h. For aromatic olefins: 2.5 mmol substrate, 5 mmol H_2O_2, 0.02 mmol Mn in 0.03 g catalyst, 5 ml acetone, 18 h. [b] A large H_2O_2 excess (600 mmol) was used; reaction time 40 h. [c] Reaction time 4 h, 80 mmol H_2O_2. [d] X = H. [e] Epoxide isomer distribution: 80% E, 20% Z. [f] $X = CH_3$.

containing faujasites, the internal space is coated with hydrophobic molecules. This strongly reduces the water affinity of the system, as evidenced e.g. by a comparison of the IR spectra of hydrated NaY and $[Mn(bpy)_2]^{2+}$–NaY. In the latter material, the intensity of the water bending vibration is strongly reduced. The *moderate hydrophobicity* of the catalytic material seems just suited for bringing together the polar oxidant and the apolar substrate.

The architecture of the original $[Mn(bpy)_2]^{2+}$–NaY system can be changed in a variety of ways. Substitution of the NaY by a NaX zeolite reduces the Brønsted acid strength, and enables the accumulation of larger epoxide yields (Table 1). For 1-hexene and cyclohexene, the selectivity increases to 81% (from 50%) and to 62% (from 6%) [5]. Another possible host material is the hexagonal faujasite with EMT topology, which is slightly more hydrophobic than the familiar NaY zeolite.

Variation of the co-cation in $[Mn(bpy)_2]^{2+}$–Y not only affects the conversion but also the selectivity of the epoxidation. Na^+ was replaced by the smaller Li^+ cation and by the larger K^+. The nature of the cation influences the siting of Mn^{2+} in the dehydrated zeolites before ligand adsorption, and may thus influence the eventual product of the ligand adsorption procedure. Moreover, for a constant cation charge of +1, a decreasing size of the cation causes a higher electrostatic potential in the zeolite voids, expectedly favoring reactions which involve highly polar transition states. Finally, the locations of these different monovalent cations in the lattice may be different.

In the sequence $K^+ \rightarrow Na^+ \rightarrow Li^+$ the activity in otherwise identical conditions increases, but the epoxide selectivity decreases [19]. With Li^+ ions, the conversion rises to 96% after 4 h against 52% after 18 h for Na^+. The least solvolysis is observed with K^+ ions, and epoxide selectivities up to 75% are obtained. Especially the latter effects on selectivity are easily understood based on the highly polar character of the epoxide solvolysis reaction. Finally, it should be stressed that presence of even limited amounts of protons can dramatically reduce epoxide selectivity. Thus exchange of the Mn zeolite at a pH of 4 causes a significant drop in epoxide yield.

On the macroscopic level, the catalyst can also be modified by incorporation in a polydimethylsiloxane (PDMS) membrane [20,21]. Operation of the catalyst then becomes possible even in the absence of a solvent, provided the substrate is able to cause some swelling of the membrane structure. Although H_2O_2 efficiencies tend to be lower with the membrane catalyst than with the free zeolite, a remarkably beneficial effect is that the use of *t*BuOOH as an oxidant becomes more favorable. These phenomena have been related to the preferential sorption of hydrophobic components in such membranes.

The replacement of bpy with phen has a profound effect on the catalytic properties of the material. The catalytic properties of Mn–phen complexes have hardly been studied to date. Recently, the aerobic oxidation of indoleacetic acid with dissolved Mn–phen complexes has been described [22]. We have investigated the catalytic properties of zeolite-entrapped Mn–phen complexes; results for oxidation of various olefins with different oxidants are summarized in Table 2. Whereas with PhIO and *t*BuOOH the highest conversions are obtained in the absence of a solvent, the use of acetone as a reaction medium is most appropriate with H_2O_2. In general the H_2O_2 conversion is considerably higher for $[Mn(phen)_2]^{2+}$–Y than for $[Mn(bpy)_2]^{2+}$–Y (e.g., 78 versus 51% for a 0.33 substrate/H_2O_2 ratio), but with bpy, oxygenation at the double bond is about 2 to 3 times more important. The considerable H_2O_2 loss to O_2 with the phen based catalyst may be due to a lesser degree of Mn complexation. We have indeed observed that free Mn, as in Mn-NaY, largely decomposes H_2O_2 via radical pathways. The latter reactions are accompanied by a small amount of alkene oxidation, mainly at the allylic position. The larger dimensions of

Table 2
Oxidation of olefins with PhIO, H_2O_2 or *t*BuOOH, catalyzed by zeolite-entrapped $[Mn(phen)_2]^{2+}$ [a]

Substrate	Oxidant	X (%)	S (%)			
			epoxide	diol	*t*BuO-ol [b]	others [c]
Cyclohexene	PhIO	15	49	—	—	51
	PhIO [d]	44	29	—	—	71
	H_2O_2	17	18	32	—	35
	*t*BuOOH	7	7	19	32	41
	*t*BuOOH [d]	18	3	28	53	16

Substrate	Oxidant	X (%)	S (%)		
			epoxide	diol	others [e]
Styrene	PhIO	13	100	—	—
	H_2O_2	16	76	2	22
	*t*BuOOH	14	67	1	32

[a] Reaction conditions: 2.5 mmol substrate; 0.5 mmol PhIO, 5 mmol H_2O_2 or 1 mmol *t*BuOOH; 20 μmol Mn (in 0.03 g catalyst), 2 ml acetone, 18 h, 293 K. [b] *t*BuO-ol = 2-*tert*-butoxycyclohexanol. [c] Products of allylic oxidation, hydration and derived products: cyclohexanol, cyclohexanone, cyclohex-2-enol, cyclohex-2-enone. [d] No solvent. [e] Mainly benzaldehyde.

the phen ligand may make the complexation less complete, causing more catalase activity on the sample. On the other hand, the $[Mn(phen)_2]^{2+}$ complexes may also themselves be at the origin of the catalase activity. It has been reported for complexes in solution that the disproportionation activity is maximal at a ligand to Mn ratio of 12 for bpy and 2 for phen [23]. The latter 2:1 phen:Mn is also present in the zeolite catalyst, suggesting a $[Mn(phen)_2]^{2+}$ contribution in the catalase activity.

Oxidation of olefins with $[Mn(phen)_2]^{2+}$–NaY and H_2O_2 mainly gives oxidation at the double bond, but hydrolysis is considerable. Moreover, side reactions for cyclohexene comprise double bond hydration to cyclohexanol and allylic oxidation to 2-cyclohexen-1-ol and 2-cyclohexen-1-one. In the case of styrene, benzaldehyde is a substantial by-product.

Using PhIO and $[Mn(phen)_2]^{2+}$–NaY, the solvolysis is negligible, and high epoxide yields are obtained. With PhIO, *cis*-$[Mn(phen)_2]^{2+}$–NaY performs even better than *cis*-$[Mn(bpy)_2]^{2+}$–Y. For styrene a selective conversion to the epoxide is seen. With cyclohexene epoxidation occurs, together with some hydration and allylic oxidation. In the reactions with *t*BuOOH epoxide selectivities are not only diminished by hydrolysis but also by formation of 2-*tert*-butoxycyclohexan-1-ol.

4.2. Tridentate ligands

The interest in the catalytic properties of Mn–triazacyclononane type complexes has arisen from their catalase-like deperoxidation activity. As these catalysts work even at room temperature, they are suited to activate bleaching processes, in which most H_2O_2 is converted into O_2 [24]. Recently it has been discovered that in the presence of an olefin, the balance between oxidant disproportionation and epoxidation can be shifted to favor the latter reaction, namely (i) by working at sub-ambient temperature, and (ii) using a solvent with which H_2O_2 reversibly forms a complex, such as acetone [25]. Moreover, it was shown that the catalytic characteristics, e.g. the activity, or the degree of stereoretention, can be influenced by changing the immediate environment of the catalytic Mn site, for instance, when alcohol or carboxylate functions are introduced into the side-chain substituents on the nitrogen atom [26]. Thus one may expect also profound differences with the solution chemistry when such catalytic species are confined to the inner pore volume of zeolites.

Tacn and tmtacn both form chelates with intrazeolite Mn, as can be proved by an analysis of the zero-field splitting in the Mn^{II} ESR spectrum [9]. Under the influence of H_2O_2, oxidized Mn^{III}–Mn^{IV} dimers are formed in both zeolites. Nevertheless the catalytic properties of the resulting materials differ dramatically. With tacn as the ligand, H_2O_2 decomposition is the main process, accompanied by very little epoxidation. With tmtacn, oxidant disproportionation is still observed, but there is an important and very selective epoxidation activity (Table 3) [27]. This difference between the two ligands may be due to the formation of hydrogen bridges be-

Table 3
Olefin oxidation with $[Mn(tmtacn)]^{2+}$–NaY and H_2O_2 [a]

Substrate	T (K)	Solvent	Conversion (%)	Epoxide sel. (%)
Styrene	298	methanol	0.4	100
	273	acetone	19.3	98
Cyclohexene	298	methanol	0.3	100
	273	acetone	25.3	95

[a] Reaction conditions: 1 mmol olefin, 1 mmol H_2O_2, 1 g of solvent, 0.025 g catalyst (containing 8 μmol Mn), 12 h.

tween the N–H groups of tacn and H_2O_2, resulting in a high local peroxide concentration at the Mn site and a pronounced peroxide decomposition. On the other hand, the secondary N–H groups of tacn are expected to be quite susceptible to oxidation, resulting in deactivation of the catalyst. This difference between the methylated and the unmethylated ligand is also observed in the corresponding homogeneous catalysis. As is observed for the homogeneous reaction, acetone is also by far the best solvent for the heterogeneous catalytic reaction. This is due to the formation of 2-hydroxy-2-hydroperoxypropane [28]:

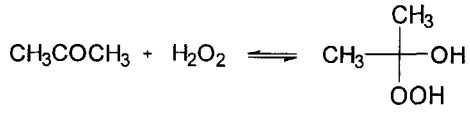

The latter compound gradually releases H_2O_2 as the reaction proceeds, maintaining a constant low oxidant concentration.

Nevertheless important differences are observed between the homogeneous $[Mn(tmtacn)]^{2+}$ catalyst and its zeolite-immobilized counterpart. First, allylic oxidation is considerably limited in comparison with the homogeneous catalyst. With the latter, some side reaction is observed, especially for aliphatic *trans* alkenes. Thus with *trans*-2-hexene, 19% of the products arise from allylic oxidation for the homogeneous catalyst. With $[Mn(tmtacn)]^{2+}$ in NaY, this value is reduced to 5%, giving an epoxide selectivity of 95% from *trans*-2-hexene. Secondly, for *cis* or *trans* aliphatic alkenes, the isomerization in the epoxide fraction is reduced with the heterogeneous catalyst in comparison with the homogeneous system. The isomer scrambling in the homogeneous catalysis probably arises from a partial radical character on the high-valent, mono-oxygen transferring Mn species. Tentatively, one may ascribe the lower degree of isomerisation in the zeolite-catalyzed reaction to a reduced molecular motion at the zeolite surface, giving less rotation around the C–C bond during the epoxidation transition state. Finally, while *trans*-2-hexene and *trans*-5-decene are about equally reactive in homogeneous catalysis, the reactivity of *trans*-5-decene is only half of that the hexene with $[Mn(tmtacn)]^{2+}$–NaY. While this may be due to a shape-selective effect, the low affinity of the very apolar decene for the polar zeolite surface undoubtedly is also important.

The acid–base situation in the $[Mn(tmtacn)]^{2+}$–NaY material deserves further comment. As with $[Mn(bpy)_2]^{2+}$–NaY, one may expect formation of acid sites after the dehydration of the zeolite, due to hydrolysis of the Mn cation. However, it was observed that one needs at least two molecules of tmtacn per Mn during the ligand adsorption in order to obtain a homogeneous distribution of the liquid ligand over the solid sample. The excess of ligand thus introduced effectively neutralizes any acidity. This contrasts with the situation in $[Mn(bpy)_2]^{2+}$–NaY; indeed bpy is a much weaker base than tmtacn, and an excess bpy has less effect on the presence of acid sites. Consequently, acid-catalyzed oxirane ring opening is hardly observed in optimum $[Mn(tmtacn)]^{2+}$–NaY catalysts. Use of only one molecule of tmtacn per Mn results in catalysts with poorer performance. For instance, the selectivity in the styrene epoxidation is reduced from over 95% (at Mn:tmtacn = 1:2), to less than 40% (at Mn:tmtacn = 1:1). Side products include benzaldehyde and phenylacetaldehyde, the latter typically resulting from acid catalysis [29].

4.3. Tetradentate Schiff bases

Schiff bases have been synthesized in an amazing structural variability. This flexibility can also be applied to optimize the design of zeolite-based hydrocarbon oxidation catalysts. The first report on this type of catalyst employed the Schiff base salen, adsorbed on a MnNaY zeolite [30]. With the resulting material, a limited number of catalyst turnovers could be obtained in the oxidation of olefins with PhIO. We extended this work to alkane oxidation, and replaced the phenol groups in the salen ligand by more oxidation-resistant pyridil groups, resulting in the pyren ligand. Whereas salen is a 3-2-3 ligand, pyren is a only 2-2-2 ligand [1]; the distances between the nitrogen donor atoms may not be sufficient to allow a planar ligand disposition around Mn. Therefore the pyrpn ligand was introduced, in which the ethylene bridge of pyren is replaced with a propylene group, resulting in a 2-3-2 ligand. Details on the synthesis and the physicochemical characteristics of the Mn Schiff base zeolites have been published [14].

In all cases, the disproportionation of H_2O_2 on the Mn Schiff base zeolites is too fast to allow use of the oxidant for oxygenation of a substrate. This catalase activity may be due to the formed complexes or to the presence of unchelated Mn. With PhIO, fair selectivities are obtained in the oxidation of cyclohexene and cyclohexane. With cyclohexene, the oxide is the main product; cyclohexane yields a cyclohexanol–cyclohexanone mixture. However, especially in the latter case, the turnover numbers are low. This is due to a combination of factors, such as the low solubility of PhIO, or the slow diffusion of PhIO in zeolite channels.

In view of the low product yields with PhIO, *t*BuOOH may be a more active alternative. With the different Mn Schiff base zeolites and olefins, styrene yields the epoxide and benzaldehyde, which is a bond fission product. That the mechanism of these oxidations is mechanistically not purely of the oxo transfer type, but at contrast has some radical character, becomes even more evident in the oxidation of cyclohexene. The mixed peroxide (cyclohex-2-enyl)(*tert*-butyl)peroxide is the main product. In his study of homogeneous [Mn(salen)] catalysis with olefins and *t*BuOOH, Kochi et al. ascribed this radical pathway to homolysis of the intermediate Mn–OO*t*Bu species, and formation of the radicals $Mn^{IV}O^{\cdot}$ and tBuO$^{\cdot}$ [31]. In homogeneous conditions, epoxide yields are improved by addition of an axially coordinating base such as pyridine. The base enables heterolysis of Mn–OO*t*Bu to $Mn^{V} = O$ and a non-radical reaction. We have tried to obtain a similar effect in the heterogeneous system via addition of pyridine, or by the use of a pentadentate ligand, such as smdptH$_2$ (bis(salicylaldehyde)methylnitrilodipropylenediimine). Such a design has been successful in the case of O_2 sorption on zeolite-entrapped Co Schiff base complexes [32]. However, in the catalysis with Mn, the homolytic pathway remained dominant, indicating that the coordination chemistry of the entrapped Mn Schiff base complexes might be different from that of the solution species.

This partial radical character however does not hinder these systems to be efficient room temperature alkane functionalisation catalysts. In a screening test (Table 4), [Mn(salen)]–NaY, $[Mn(pyren)]^{2+}$–NaY and $[Mn(pyrpn)]^{2+}$–NaY display a comparable activity in cyclohexane oxygenation, with yields about 10 times higher than with PhIO. However, a clear difference between the different catalysts emerges when reactions are conducted over longer periods, and at lower catalyst concentration. In the long run, the catalysts with the pyren or pyrpn ligand remain active, while with the salen ligand fast deactivation occurs. This contrast is most likely due to the presence of the phenol group in salen, which is susceptible to oxidation [33].

[1] The digits refer to the number of C atoms linking the coordinating N or O atoms.

Table 4
Alkane and olefin oxidation with Mn Schiff base zeolites and different oxidants [a]

Substrate	Catalyst	Oxidant	Products (mol per mol Mn)		
			epoxide	enone [b]	peroxide [c]
Cyclohexene	[Mn(salen)]–NaY	PhIO	3.5	1.1	—
	$[Mn(pyren)]^{2+}$–NaY	PhIO	1.4	1.0	—
	[Mn(salen)]–NaY	*t*BuOOH	0.2	2.5	12.1
	$[Mn(pyren)]^{2+}$–NaY	*t*BuOOH	0.5	2.1	10.8
Substrate	Catalyst	Oxidant	Products (mol per mol Mn)		
			epoxide	PhCOH	
Styrene	[Mn(salen)]–NaY	PhIO	13.3	1.1	
	$[Mn(pyren)]^{2+}$–NaY	PhIO	9.8	4	
	[Mn(salen)]–NaY	*t*BuOOH	3.0	3.7	
	$[Mn(pyren)]^{2+}$–NaY	*t*BuOOH	2.7	2.5	
	$[Mn(pyrpn)]^{2+}$–NaY	*t*BuOOH	2.5	3.6	
Substrate	Catalyst	Oxidant	Products (mol per mol Mn)		
			alcohol	ketone	
Cyclohexane	[Mn(salen)]–NaY	PhIO	0.55	0.5	
	$[Mn(pyren)]^{2+}$–NaY	PhIO	0.65	0.5	
	[Mn(salen)]–NaY	*t*BuOOH	1.0	4.2	
	$[Mn(pyren)]^{2+}$–NaY	*t*BuOOH	3.2	7.7	
	$[Mn(pyrpn)]^{2+}$–NaY	*t*BuOOH	2.4	7.3	
[d]	[Mn(salen)]–NaY	*t*BuOOH	5.3	8.0	
[d]	$[Mn(pyren)]^{2+}$–NaY	*t*BuOOH	6.1	70.5	
[d]	$[Mn(pyrpn)]^{2+}$–NaY	*t*BuOOH	6.7	50.0	

[a] Reaction conditions: 2.5 mmol substrate; 1 mmol PhIO in 2 ml acetonitrile or 1.5 mmol *t*BuOOH in 2 ml acetone; 30 μmol Mn in 0.1 g catalyst, 293 K, 10 h. [b] Enone = 2-cyclohexen-1-one. [c] Peroxide = (cyclohex-2-enyl)(*t*-butyl)peroxide. [d] Conditions: 50 mmol cyclohexane, 80 mmol *t*BuOOH, 50 ml acetone, 150 μmol Mn in 0.5 g catalyst, 293 K, 50 h.

$[Mn(pyren)]^{2+}$–NaY does not contain this oxidation-sensitive site; and high oxidate yields are obtained, up to 2.5 g of oxidate per g of catalyst, which is the same as for the well-studied Fe–phthalocyanine in NaY catalyst [34]. On a Mn basis, the minimum turnover number is 150. The ketone selectivities are remarkably high: in one step 90% ketone is obtained from the alkane.

The heterogeneity of these systems deserves a special comment. At contrast with the previously discussed neutral bidentate and tridentate ligands, tetradentate Schiff bases such as salen, or the tetradentate amide ligands, may loose protons upon chelation, and the resulting complexes may be neutral. We have observed that for neutral complexes such as [Mn(salen)]–NaY, leaching of the complexes into solution may occur, especially if the catalytic reaction is performed in a highly polar solvent. Such problems can be overcome (i) by Soxhlet extracting the catalyst at the end of the synthesis with a rather polar solvent, e.g. acetone, and (ii) by subsequently performing the reaction in a less polar solvent such as dichloromethane. Thus the

Table 5
Oxidation of cyclohexene with H_2O_2, catalyzed by [Mn(bpen)]–NaY and [Mn(bppn)]–NaY.

Catalyst	*X* (%)	*S* (%)		
		epoxide	diol	dione
[Mn(bppn)]–Y	96	36	50	11
[Mn(bpen)]–Y	73	7.5	78	12

Reaction conditions: 2.5 mmol cyclohexene, 20 mmol H_2O_2 (as a 35% aqueous solution), 293 K 0.05 g catalyst (containing 3 μmol Mn), in 2 g acetone. In both reactions, small amounts of cyclohexanone and 2-cyclohexen-1-one were detected (respectively 1 and 2%).

catalysis occurs under truly heterogeneous conditions. The complexes formed from Mn and pyren or pyrpn at contrast are cationic, and their retention in the zeolite framework is superior to that of the salen complexes. This constitutes another advantage of these modified Schiff base ligands.

4.4. Tetradentate amide ligands

The family of the amide ligands constitutes a further possibility for structural variation. As an example, Table 5 presents results obtained with H_2O_2 and Mn zeolites containing the ligands bpen and bppn. When excesses of H_2O_2 are used, high conversions of cyclohexene can be obtained, with predominantly double bond oxidation. Conversions and epoxide selectivities are somewhat higher for bppn than for bpen containing catalysts. Our data allow a comparison with the homogeneous catalysis by Mn complexes of related diamido ligands, reported by Leung et al. [35]. The homogeneously catalyzed cyclohexene oxidation with [Mn(bpc)(O_2CMe)] (bpc = 4,5-dichloro-1,2-bis(pyridine-2-carboxamido)-benzene) gives an epoxide yield of 44% and cyclohex-2-en-1-one and -1-ol yields of 24% and 11% respectively. In the heterogeneous, zeolite-catalyzed reactions far less allylic oxidation occurs. This observation parallels what happens with the tmtacn catalysis upon immobilisation in a zeolite.

5. Glossary

bpen	*N*,*N*′-bis(2-pyridinecarboxamide)-1,2-ethane
bppn	*N*,*N*′-bis(2-pyridinecarboxamide)-1,3-propane
bpy	2,2′-bypiridine
phen	phenantroline
pyren	bis(2-pyridinecarboxaldehyde)-1,2-ethylenediimine
pyrpn	bis(2-pyridinecarboxaldehyde)-1,3-propylenediimine
salenH_2	bis(salicylaldehyde)ethylenediimine
tacn	1,4,7-triazacyclononane
tmcyclam	1,4,8,11-tetramethyl-1,4,8,11-tetra-azacyclotetradecane
tmtacn	1,4,7-trimethyl-1,4,7-triazacyclononane
trien	triethylenetetramine

Acknowledgements

We are indebted to the Belgian federal government for support in the frame of an Inter-Universitary Attraction Pole on Supramolecular Catalysis. PPKG and DDV thank the Belgian National Fund for Scientific Research (N.F.W.O.) for fellowships as research assistant and post-doctoral researcher.

References

[1] V.L. Pecoraro, M.J. Baldwin and A. Gelasco, Chem. Rev. 94 (1994) 807; K. Wieghardt, Angew. Chem. Int. Ed. Engl. 28 (1989) 1153; G.W. Brudvig and R.H. Crabtree, Prog. Inorg. Chem. 37 (1989) 99; V.L. Pecoraro, (Ed.), Mn Redox Enzymes (Verlag Chemie, New York, 1992).
[2] H.J. Eppley, H. Tsai, N. de Vries, K. Folting, G. Christou and D.N. Hendrickson, J. Am. Chem. Soc. 117 (1995) 301.
[3] G. Christou, Acc. Chem. Res. 22 (1989) 328.
[4] D.J. Barnes, R.L. Chapman, F.S. Stephens and R.S. Vagg, Inorg. Chim. Acta 51 (1981) 155.
[5] P.P. Knops-Gerrits, D.E. De Vos, F. Thibault-Starzyk and P.A. Jacobs, Nature 369 (1994) 543.
[6] B. Bleaney and D.J.E. Ingram, Proc. R. Soc. London A 205 (1951) 336; R.D. Dowsing, J.F. Gibson, D.M. Goodgame, M. Goodgame and P.J. Hayward, Nature 219 (1968) 1037.
[7] T.I. Barry and L.A. Lay, Nature 208 (1965) 1312; J. Phys. Chem. Solids 27 (1966) 1821; Nature 29 (1968) 1395.
[8] H.W. De Wijn and R.F. Van Balderen, J. Chem. Phys. 46 (1967) 1381.
[9] D.E. De Vos and T. Bein, submitted for publication.
[10] G.M. Woltermann and J.R. Wasson, Inorg. Chem. 12 (1973) 2366.
[11] S.R. Cooper and M. Calvin, J. Am. Chem. Soc. 99 (1977) 6623; S.R. Cooper, G.C. Dismukes, M.P. Klein and M. Calvin, J. Am. Chem. Soc. 100 (1977) 7248.
[12] A. Lever, Inorganic Electronic Spectroscopy, 2nd Ed. (Elsevier, 1984).
[13] W.R. McWhinney and J.D. Miller, Adv. Inorg. Chem. Radiochem. 12 (1967) 135; P.P. Knops-Gerrits, F. De Schryver,

H. Van Mingroot, M. Van der Auweraer, X.Y. Li and P.A. Jacobs, Chem. Eur. J. 2 (1996) 592.
[14] D.E. De Vos, P.P. Knops-Gerrits, D.L. Vanoppen and P.A. Jacobs, Supramol. Chem. 6 (1995) 49.
[15] E.D. McKenzie, Coord. Chem. Rev. 6 (1971) 187.
[16] V.K. Kaushik, S.G.T. Bhat and D.R. Corbin, Zeolites 13 (1993) 671.
[17] P.P. Knops-Gerrits, P.A. Jacobs, X.Y. Li and N.T. Yu, Proc. 14th Int. Conf. Raman Spectrosc. (Wiley Interscience, 1994) B-165.
[18] P.P. Knops-Gerrits, F. Thibault-Starzyk and P.A. Jacobs, Stud. Surf. Sci. Catal. B 84 (1994) 1411.
[19] P.P. Knops-Gerrits, H. Toufar and P.A. Jacobs, Stud. Surf. Sci. Catal. (1996), in press.
[20] P.P. Knops-Gerrits, I. Vankelekom, E. Béatse, P.A. Jacobs, Catal. Today (1996), in press.
[21] R. Parton, I. Vankelecom, D. Tas, K. Janssen, P.P. Knops-Gerrits and P.A. Jacobs, J. Mol. Catal. (1996), in press.
[22] R. Pressey, J. Mol. Catal. 70 (1991) 243.
[23] Y.D. Tiginyanu, A.Y. Sychev and V.M. Berdnikov, Russ. J. Phys. Chem. 45 (1971) 975, 1434.
[24] R. Hage, J.E. Iburg, J. Kerschner, J.H. Kock, E.L.M. Lempers, R.J. Martens, U.S. Racherla, S.W. Russell, T. Swarthoff, M.R.P. van Vliet, J.B. Warnaar, L. van der Wolf and B. Krijnen, Nature 369 (1994) 637.
[25] D.E. De Vos and T. Bein, J. Chem. Soc. Chem. Commun. (1996) 917.
[26] D.E. De Vos and T. Bein, J. Organomet. Chem. (1996) in press.
[27] D.E. De Vos, J. Meinershagen and T. Bein, Angew. Chem. (1996), in press.
[28] M.V.C. Sauer and J.O. Edwards, J. Phys. Chem. 75 (1971) 3004.
[29] D.E. De Vos, J. Meinershagen and T. Bein, Proc. XIth Int. Conf. Catal. (1996), in press.
[30] C. Bowers and P.K. Dutta, J. Catal. 122 (1990) 271.
[31] K. Srinivasan, S. Perrier and J.K. Kochi, J. Mol. Catal. 36 (1986) 297.
[32] D.E. De Vos, E.J. Feijen, R.A. Schoonheydt and P.A. Jacobs, J. Am. Chem. Soc. 116 (1994) 4746.
[33] D. Hamilton, R.S. Drago and A. Zombeck, J. Am. Chem. Soc. 109 (1987) 374.
[34] R.F. Parton, L. Uytterhoeven and P.A. Jacobs, Stud. Surf. Sci. Catal. 59 (1991) 395.
[35] W.H. Leung, J.-X. Ma, V.W.-W. Yam, C.-M. Che and C.-K. Poon, J. Chem. Soc. Dalton Trans. 1071 (1991).